

## Radiation Distribution During Impurity Seeding Experiments in the Full Tungsten ASDEX Upgrade

J.C. Fuchs, T. Eich, L. Giannone, A. Herrmann, A. Kallenbach, B. Reiter,  
and the ASDEX Upgrade Team

Max-Planck-Institut für Plasmaphysik, EURATOM Association, Garching, Germany

### Introduction

Since 2007 all plasma facing components (PFCs) in ASDEX Upgrade are coated with tungsten in order to investigate the plasma wall interaction and its implications in an all tungsten divertor tokamak, i.e. in absence of carbon. With the first boronisation after more than one year of operation with full-W coating, the intrinsic radiation level dropped and the power load at the divertor target increased such that the power flux could exceed the power limits of a few target tiles with thick vacuum plasma sprayed (VPS) coating. Therefore operation at high heating powers was possible only with radiative cooling, which was achieved by feedback-controlled injection of nitrogen using thermoelectric current measurements in the outer divertor. This resulted not only in the desired divertor power load reduction, but also in improved energy confinement.<sup>[1]</sup>

The key player in order to reduce the power load on the divertor plates is the control of the divertor radiation. The radiation in ASDEX Upgrade discharges is routinely measured by up to 104 bolometers mounted in several cameras at different poloidal positions in one toroidal position. From the measured line integrals the total radiated power can be determined and the distribution of the radiation emissivity is reconstructed in the divertor and X-point region as well as in the main plasma by deconvolution methods.

### Radiation distribution during nitrogen seeding

It was found that in discharges with unboronised, full tungsten covered PFCs the radiated power was about 60% of the input power, which was comparable to configurations with mixed tungsten and carbon covered PFCs, however in the full tungsten device there is clearly less radiation from the X-point and divertor region than in discharges with mixed tungsten and carbon coated PFCs, whereas the radiation from the main plasma and the edge has increased.<sup>[2]</sup>

After boronisation in the full tungsten device the radiation level has clearly decreased due to the reduced number of radiating intrinsic impurities, both in the divertor region, but most significantly in the main cham-

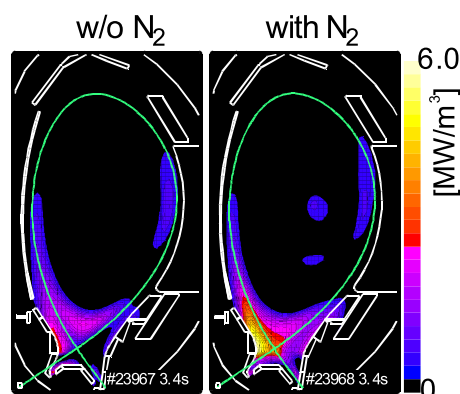


Fig 1: Distribution of the radiation emissivity in a poloidal cross section of ASDEX Upgrade for two discharges with similar plasma parameters: one reference discharge without impurity injection (left), and one discharge with nitrogen seeding (right).

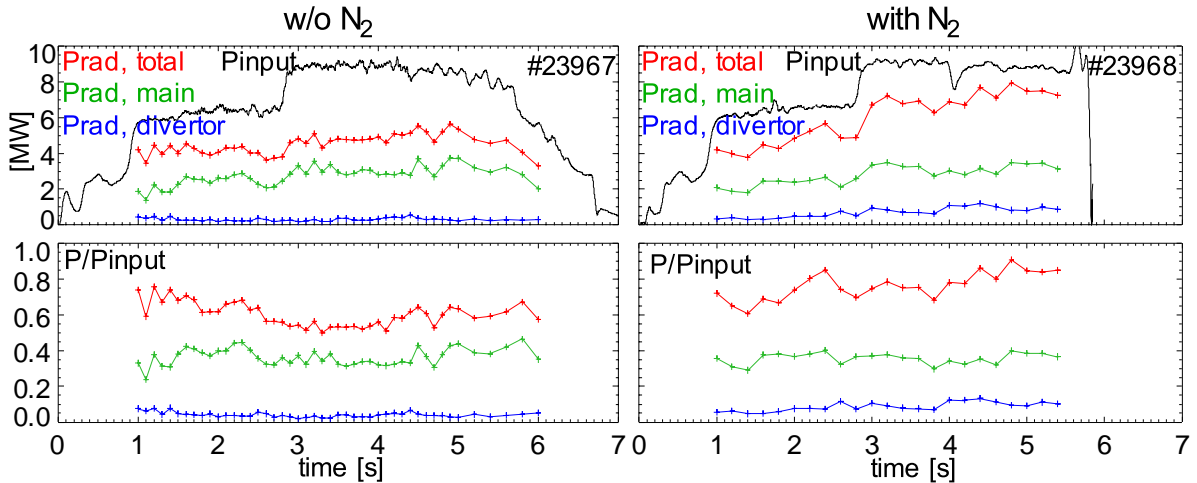


Fig. 2: Time evolution of the radiated power for a reference discharge without impurity seeding (left) and a nitrogen seeded discharge (right). Plotted are the the input power (black), the total radiated power (red), the radiated power in the main plasma (green) and in the divertor (blue) as total values (top) and as fractions of the input power (bottom).

ber.<sup>[3]</sup> In order to avoid too high power fluxes to the divertor, radiative cooling was achieved by feedback controlled injection of impurities from various local positions.

Figure 1 shows a comparison of the distribution of the radiation emissivity in a poloidal cross section of ASDEX Upgrade with boronised, full tungsten walls for two discharges with 1MA plasma current, 9 MW additional heating power (7.5 MW neutral beam injection, 1.5 MW ECRH) and a fractional Greenwald density of  $n_e/n_{GW} \sim 0.65$ . The first plot is for a reference discharge without any impurity seeding, the second one for a discharge with feedback controlled nitrogen seeding using thermoelectric current measurements in the outer divertor. Integrating the radiation emissivity over the whole plasma volume or parts of it gives the total radiated power and the radiated power e.g. from the divertor or the core plasma. Time traces of these values for the two discharges from figure 1 are plotted in figure 2 both as absolute values (top) and as fractions of the input power (bottom).

Whereas in the unseeded discharge we find a total radiated power of about 60% of the input power, the radiation level in the nitrogen seeded discharge increased as expected to a level of about 80% of the input power, however the distribution of the radiation has changed significantly: the increase of the total radiated power is mainly caused by the increased radiation from the X-point and divertor region, which raised from ELM averaged local emissivities of 2-3 MW/m<sup>3</sup> in unseeded discharges to more than 6 MW/m<sup>3</sup> in nitrogen seeded discharges, which is comparable to former campaigns with mixed carbon and tungsten PFCs. Correspondingly the integrated radiated power from the X point and divertor re-

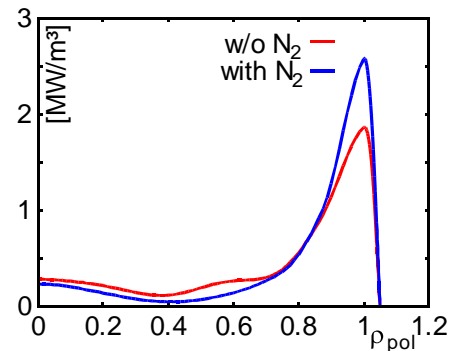


Fig. 3: Radiation emissivity in the main plasma as a function of the normalised radius  $\rho_{pol}$  for the two discharges from figure 1.

gion has increased by more than a factor of two from 5-10% of the input power to 15-20%.

There is also an increase of radiation from the edge of the main plasma: Figure 3 shows a comparison of one dimensional radiation profiles as a function of the normalised radius  $\rho_{\text{pol}}$  for the two shots from figure 1, calculated by an Abel inversion under the assumption of constant emissivities on flux surfaces, using only those bolometer lines of sight which are looking through the upper half of the main plasma. A slight increase of the edge radiation can be seen in the case of the nitrogen seeded discharge, however this increase is not as large as the increase of the divertor radiation, and it is not illustrated in figure 1 where the colour scale is optimized for displaying the dominant divertor radiation.

### Power balance

Subtracting the total radiated power measured by bolometers, the power load on the divertor targets measured by IR cameras, and the change of the MHD energy of the plasma from the input power and taking into account that parts of the divertor radiation are recorded by both bolometers and IR cameras, one arrives at a reasonable good power balance for both unseeded discharges and discharges with nitrogen injection, as shown in figure 4 for the two discharges from figure 1. It can clearly be seen that with the increased radiation during nitrogen injection the ELM averaged power load to the divertor targets is considerably reduced as desired.

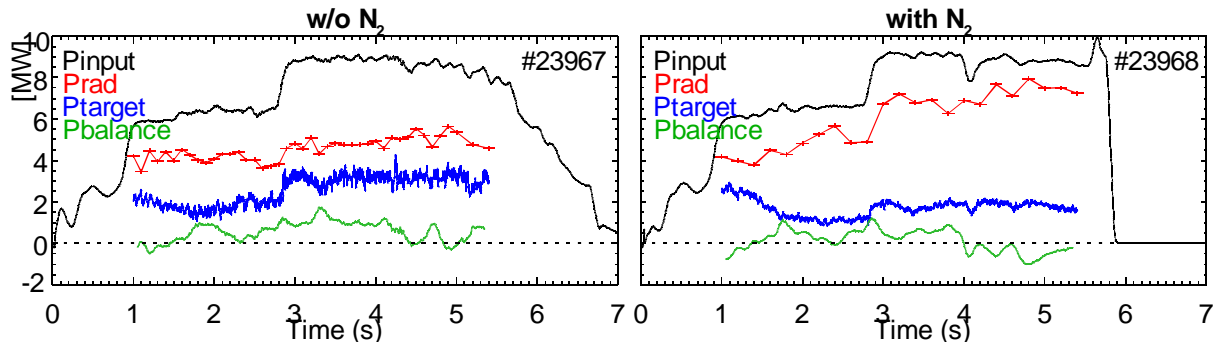


Fig. 4: ELM averaged power balance for the two discharges from figure 1, showing the input power (black), total radiated power measured by bolometers (red), power load to the divertor target tiles measured by IR cameras (blue) and the power balance (green).

### Radiation and power balance during type-I ELMs with nitrogen seeding

By using the accumulated energy on a bolometer foil instead of the momentarily absorbed power one can investigate radiation energy losses due to type-I ELMs.<sup>[5]</sup> Figure 4 shows for a number of type-I ELMs from discharges with and without nitrogen seeding in the boronized full tungsten machine the dependence of the normalized ELM radiation  $\Delta E_{\text{rad,ELM}}/E_{\text{ELM}}$  on the ELM energy  $E_{\text{ELM}}$ . Typically for unseeded discharges about 20% of the ELM energy are found as radiation. For nitrogen seeded discharges however the ELM energy is smaller, and about 40% of this energy is radiated, this value is comparable to that found in former campaigns with mixed carbon and tungsten PFCs.<sup>[5]</sup> The increase of the radiated fraction of the ELM energy is due to the decreased ELM energy, whereas the absolute radiated energy due to an ELM is nearly the

same for both seeded and unseeded discharges. Consequently, the power load to the divertor targets during a type-I ELM drops significantly with nitrogen seeding.

The newly installed AXUV photodiodes allow to measure the plasma radiation with a time resolution of 500kHz.<sup>[4]</sup> Therefore, after calibrating their measured line integrals with the absolute values measured by the foil bolometers, also a reconstruction of the radiation distribution during ELMs is possible. Figure 6 shows the distribution of the additional radiation due to a type-I ELM for a discharge with 7 MW of additional heating power in the unboronised, full tungsten machine without impurity seeding. The highest radiation emissivities are found near the inner divertor, however due to the larger volume most of the ELM radiation comes from the main plasma near the X point region, which is compatible to the radiation distribution found in ASDEX Upgrade after all PFCs have been covered with tungsten.<sup>[2]</sup> A more detailed analysis of the ELM radiation is in progress.

#### Seeding at other positions and other impurities

Figure 7 shows radiation profiles in the divertor region of comparable discharges without any impurity seeding, with nitrogen seeding from the divertor or in the midplane, and with neon seeding. All these shots behaved somewhat similar, the best results concerning power load reduction and confinement have been achieved with feedback controlled injection of nitrogen into the divertor.

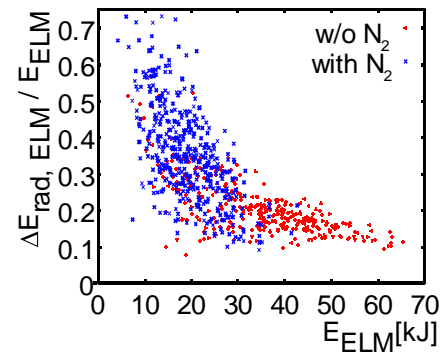


Fig. 5: Distribution of the normalized radiated energy due to a type-I ELM  $\Delta E_{rad,ELM}/E_{ELM}$  as a function of the ELM energy, with (blue) and without (red) nitrogen seeding

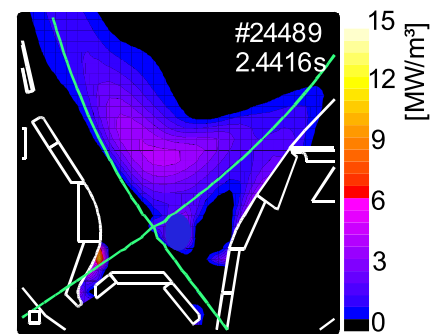


Fig. 6: Additional radiation due to an type-I ELM in an unseeded discharge

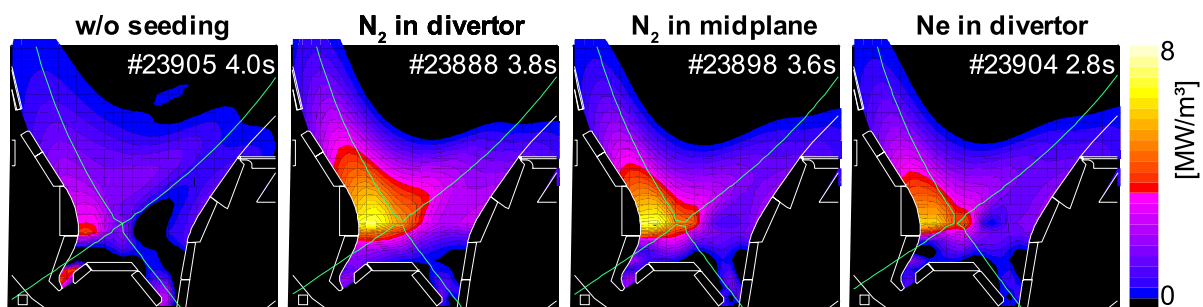


Fig. 7: Radiation distribution in the divertor for comparable discharges without any impurity seeding, with nitrogen seeding in the divertor or midplane, and with neon seeding.

#### References

- [1] O. Gruber et. al., to be published in *Nuclear Fusion*
- [2] J.C. Fuchs et. al. *Europhysics Conference Abstracts* **32D** (2008) P2.012
- [3] A. Kallenbach et. al., *Nuclear Fusion* **49** (2009) 045007
- [4] B. Reiter et. al., this conference, P1.161
- [5] J.C. Fuchs et. al., *Journal of Nuclear Materials*, **337-339** (2005), 756